Zinc is involved in depression by modulating G-protein-coupled receptor heterodimerization

Mercè Tena-Campos[1], Eva Ramon[1], Cecylia S. Lupala[2], Juan J. Pérez[2], Karl-W. Koch[3] and Pere Garriga[1]

[1]Departament d'Enginyeria Química, Grup de Biotecnologia Molecular i Industrial, Centre de Biotecnologia Molecular, Universitat Politècnica de Catalunya, Edifici Gaia, Rambla de Sant Nebridi 22, 08222 Terrassa, Catalonia, Spain.

[2]Departament d'Enginyeria Química, Centre de Biotecnologia Molecular, Universitat Politècnica de Catalunya, ETSEIB, Avda. Diagonal 647, 08028 Barcelona, Catalonia, Spain.

[3]Department of Neurosciences, Biochemistry group, University of Oldenburg, Carl-von-Ossietzky-Str. 9-11 D-26129 Oldenburg, Germany.

Address correspondence: Pere Garriga, Centre de Biotecnologia Molecular, Departament d'Enginyeria Química, Universitat Politècnica de Catalunya, Rambla de Sant Nebridi 22, 08222 Terrassa, Spain. Tel: +34 937398568; Fax: +34 937398225; E-mail: pere.garriga@upc.edu

Abstract

5-Hydroxytryptamine 1A receptor and galanin receptor 1 belong to the G-protein-coupled receptors superfamily and they have been described to heterodimerize triggering an anomalous physiological state that would underly depression. Zinc supplementation has been widely reported to improve treatment against major depressive disorder. Our work has focused on the study and characterization of these receptors and its relationships with zinc both under purified conditions and in cell culture. To this aim, we have designed a strategy to purify the receptors in a conformationally active state. We have used receptors tagged with the monoclonal Rho-1D4 antibody, and employed ligand assisted purification in order to successfully purify both receptors in a properly folded and active state. The interaction between both purified receptors has been analyzed by surface plasmon resonance in order to determine the kinetics of dimerization. Zinc effect on heteromer has also been tested using the same methodology, but exposing the 5-hydroxytryptamine 1A receptor to zinc before the binding experiment. These results, combined with FRET measurements, in the absence and presence of zinc, suggest that this ion is capable of disrupting this interaction. Moreover, molecular modelling suggests that there is a coincidence between zinc binding sites and heterodimerization interfaces for the serotonin receptor.

Our results establish a rational explanation for the role of zinc in the molecular processes associated with receptor-receptor interactions and its relationship with depression, in agreement with previously reported evidence for the positive effects of zinc in depression treatment, and the involvement of our target dimer in the same disease.

Keywords: G-protein-coupled receptor, heterodimerization, protein stability, purified receptor, galanin receptor, serotonin receptor, G-protein signaling, zinc, depression

Introduction

5-Hydroxytryptamine receptor 1A (5-HT_{1A}) belongs to class A of G-protein coupled receptors (GPCRs) superfamily [1] and plays an important role in mediating mood effects in the brain where it is found at high concentrations in the hippocampus, lateral septum, cortical areas and the mesencephalic raphe nuclei [2]. Functionally, 5-HT_{1A} underlies the molecular mechanism of major depressive and anxiolytic disorders [3]. Its signaling mechanism involves binding and activating the heterotrimeric G-protein G_i/G_0. 5-HT_{1A} has been reported to homo and heterodimerize with other GPCRs [4,5], although the details and the physiological role of these interactions have not yet been fully elucidated. 5-HT_{1A} heterodimerization with the galanin 1 receptor ($GalR_1$) has been recently reported [6]. $GalR_1$ belongs to the same family of GPCRs that 5-HT_{1A}, and interacts with the same G-protein subtype but in this case it is widespread throughout the human body, particularly in brain, spinal cord, small intestine and pancreas [7]. $GalR_1$ is becoming increasingly the focus of interest because of its potential role in a number of different pathological states with high prevalence in our society, like nicotine dependence [8,9] status epilepticus [10] and cancer [11]. In addition, it has also been involved in major depressive disorder by modulating 5-HT_{1A} functionality via specific heterodimerization with this serotonin receptor [6]. This interaction would antagonize 5-HT_{1A} neurotransmission, and $GalR_1$ antagonists could act as effective antidepressant drugs [12]. Although this interaction has only been demonstrated recently, it was first suggested more than two decades ago [13]. On the other side, zinc has also been proposed to be associated with depressive disorder [14] and this could be mediated by its interaction with the 5-HT_{1A} receptor. Clinical studies have shown that zinc supplementation increases the efficiency of the 5-HT_{1A} receptor ligands citalopram and imipramine used in depression treatment [15,16]. Moreover, zinc has been associated with other GPCRs, for example being the agonist for the GPR39 receptor [17], another GPCR also linked with depressive disorder [18]. Based on the established link between zinc and 5-HT_{1A}, and of this receptor with $GalR_1$, we hypothesized that zinc could be involved in altering the heterodimerization process between 5-HT_{1A} and $GalR_1$.

In order to test this hypothesis we have undertaken a detailed characterization of the heterodimerization process of these two receptors by means of spectroscopic methods. We set up to perform this characterization by means of surface plasmon resonance (SPR) spectroscopy. To this aim we have purified the receptors by Rho-1D4 immunopurification in the presence of ligand, and analyzed in detail its molecular properties by UV-visible and fluorescence spectroscopy and immunofluorescence

detection. We have determined that the purified receptors are in a correctly folded functional state. Furthermore, we have been able to follow the specific kinetic features of the dimerization process of the purified receptors in real time for the first time by using SPR, and more importantly we have found that zinc impairs the heterodimerization process of these receptors. These results have also been confirmed *in vivo* by Förster resonance energy transfer (FRET) spectroscopy measurements of cells expressing the two receptors. Taken together these results suggest that the heterodimerization process is regulated by zinc.

Materials and methods

Receptor expression and characterization

Plasmid constructs. Rho-1D4 tag is a specific sequence of the bovine visual GPCR rhodopsin that corresponds to the epitope for the monoclonal Rho-1D4 antibody. This tag was added, at the C-terminus, by inverse PCR to the expression vectors pCDNA3.1 contaning either $GalR_1$ or 5-HT_{1A} genes (Missouri S&T cDNA Resource Center, US), using the following primers: Fw: 5' ACGGAGACGAGCCAGGTGGCCCCGGCCTGACTCGAGTCTAGAGGGCC 3' and Rv: 5' GGCCGGGGCCACCTGGCTCGTCTCCGTCACATGAGTACAATTGGTTG3'- for $GalR_1$ gene and Fw: 5' ACGGAGACGAGCCAGGTGGCCCCGGCCTGACTCGATAGAGGGCCCG 3' and Rv: 5'GGCCGGGGCCACCTGGCTCGTCTCCGTCTGGCGGCAGAACTTACACT for 5-HT_{1A} gene. Resulting constructs were sequenced to check both appropriate tag addition and unspecific mutation absence (Stabvida, Portugal). p5-HT_{1A}-ECFP and p$GalR_1$-EYFP constructs were kindly provided by Dr. Borroto-Escuela (Karolinska Institute, Sweden) and pECFP-EYFP was obtained by subcloning PCR amplified EYFP onto the pECFP empty vector.

Protein expression and purification. The constructs were transiently transfected into HEK-293S GnTi$^-$ cells (EACC, UK) using polyethylenimine (Polysciences, Germany) as previously described [19]. This cell line was used because it lacks glycosylation and allows a better visualization of the protein bands in electrophoretic gels. Cells were routinely grown in DMEM-F12 media (Labclinics, Spain) supplemented with 10% FBS, penicillin-streptomycin (100u/ml) and 2mM L-glutamine (Sigma, Spain) at 37ºC and 5% CO_2 atmosphere. For protein purification cells were harvested 48h after transfection and pelleted at 4000g during 20min. The pellet was then solubilized in 10 ml per harvested plate in tris buffered saline (TBS) containing 2% Triton X-100, 100μM phenylmethylsulfonyl fluoride and 1μM of

receptor agonist, galanin 1-29 (Sigma, Spain) for $GalR_1$ receptor and 8-OH-DPAT (Tocris, UK) for 5-HT_{1A}, at 4ºC during 1h. Solubilized cells were centrifuged at 35000rpm for 35min at 4ºC and the supernatant was incubated by gently nutating with CNBr-activated Sepharose 4B Fast Flow (GE healthcare, Spain) coupled to Rho-1D4 antibody (Cell Essentials, US) during 2.5h. The sepharose beads were recovered and washed with 50mM MES buffer, pH 6.0 (Sigma, Spain) containing 0.05% dodecyl maltoside (DM) (Anatrace, UK) for five times. Elution was performed during 3h with 50mM MES buffer pH 6.0 containing 0.05% DM and 0.5mM Rho-1D4 9-mer peptide (TETSQVAPA) (Unitat de Tècniques Separatives i Síntesi de Pèptids, Universitat de Barcelona, Spain).

Purified protein quantification. Protein spectra were recorded using Cary100 UV-vis spectrophotomer (Cary, Australia) between 250nm and 350nm. Then, purified protein concentration was calculated using receptors extinction molar coefficient, obtained from ProtParam with accession numbers P08908 for 5-HT_{1A} and P47211 for $GalR_1$ respectively**.**

Blue-native PAGE. 2μg of each purified receptor were mixed with native loading buffer (5% glycerol, 0.04% ponceau red in water) and were loaded into tricine (Sigma, Spain) blue native PAGE gel (3-14%), as described previously [20]. The gel was run for 4h at 100V and room temperature (RT), using two different proteins standards; bovine serum albumin (BSA) (Sigma, Spain) and the protein ladder NativeMark™ Unstained Protein Standard (Life technologies, US).

Western Blot. 500ng of each receptor were mixed with denaturing loading buffer and loaded onto an SDS-PAGE gel (3-14%). The gel was run for 40min at 250V in Laemmli running buffer and using SDS7B2 pre-stained marker (Sigma, Spain) as a protein standard. The proteins were subsequently transferred onto a nitrocellulose membrane (Sigma, Spain), blocked with blocking buffer (5% skimmed milk in tris buffered saline buffer (TBS)) and incubated with Rho-1D4 (dilution 1:10000 from stock) as primary antibody and anti-mouse IgG conjugated to horseradish peroxidase as secondary antibody (Santa Cruz Biotechnology, USA) in TBS. The blots were developed using substrate SuperSignal West Pico Chemiluminiscent Substrate (Luminol/H_2O_2) (ThermoFisher Scientific, France).

Immunofluorescence Microscopy. Cells were seeded in glass coverslips for 24 h and transfected with pCDNA3.1+-$GalR_1$-1D4 and pCDNA3.1+-5-HT_{1A}-1D4 using polyethylenimine as described above. One day after transfection, cells were washed with phosphate buffered saline (PBS) (Sigma, Spain) and fixed with formalin (Sigma, Spain) for 20 min. After washing twice with PBS, cells were blocked with blocking buffer during 1 h at RT. Then cells were incubated with the Rho-1D4 antibody (dilution

1/2000 from stock) for 30min at RT, washed with TTBS (TBS containing 0.1% tween-20 (Sigma, Spain)) and incubated with anti-mouse FITC (dilution 1/200 from stock) (Sigma, Spain) during 1h more. Coverslips were mounted using Vectashield Mounting medium with DAPI (Vector Labs, UK). Cell images were taken by inverted fluorescence microscopy using Nikon Eclipse Ti microscope (Isaza, Spain).

Protein stability assay. Purified proteins at a concentration of 1μM or L-Trp (12μM) were exposed to dithiothreitol (DTT) (Sigma, Spain) using different concentrations (0, 1.5, 3, 4.5, 6 and 10mM) for 15min and the proteins were subsequently exposed to 6M of guanidine hydrochloride (GndHCl) (Fisher Scientific, France) for 30 min at RT. Protein intrinsic fluorescence spectra was measured at RT on a QuantaMaster 4 spectrofluorimeter (PTI, USA), using 295nm as excitation wavelength (to minimize the contribution of tyrosine fluorescence) and 310nm-400nm as emission wavelength range. Spectra where corrected for background fluorescence from buffer, DTT and GndHCl. Data were smoothed using PeakFit (Systat Software, USA) and normalized using the same software.

G-protein activation assay. For activation experiments, purified Gα subunits, Gαi1 and Gαi2, were purchased from Prospec (Ness Ziona, Israel). Purified 5-HT_{1A} and $GalR_1$ activities were tested by measuring Gαi2 and Gαi1 activation, respectively. Since receptors were purified bound to their agonist, activation measurements were performed using PTI spectrofluorimeter by monitoring G-protein intrinsic fluorescence before and after addition of GTPγS. The spectrofluorimeter settings were 280nm as excitation wavelength and 338nm as emission wavelength. Experimental conditions were: 5nM receptor, 100nM Gα subunit, 25mM Tris pH 7.5, 100mM NaCl, 5mM $MgCl_2$, 2.5mM DTT, 0.06% DM. 30μM GTPγS was added to the sample after waiting for spectral stabilization.

Heterodimerization assays in cells and in purified system

FRET assays. HEK293T cells were transiently co-transfected as explained above in six well plates with the p5-HT_{1A}-ECFP and p$GalR_1$-EYFP vectors at a 1:1 ratio and pCFP-EYFP in DMEM media (Sigma, Spain) supplemented with 10% FBS, penicillin-streptomycin (100u/ml), 2mM L-glutamine and different zinc chloride ($ZnCl_2$) concentrations (0, 50, 100 and 200μM). pECFP-EYFP transfected wells were used as negative controls. Two days after transfection cells were harvested and resuspended in PBS containing $0.1g{\cdot}l^{-1}$ $CaCl_2$, $0.1g{\cdot}l^{-1}$ $MgCl_2$ and $0.1g{\cdot}l^{-1}$ D-glucose (Sigma, Spain). Then cells were seeded onto 96-well black plates. Cell concentration was adjusted by means of protein quantification kit (Fluka, Spain). Finally, FRET spectra were measured using an Infinite M200 plate reader (Tecan,

Switezerland). Excitation wavelength was set at 410nm and emission was recorded from 455 to 560 nm. Data was smoothed and normalized by using PeakFit.

Protein-protein interaction analysis by SPR spectroscopy

Sensorchip preparation. SPR experiments were performed using Biacore 2000 (GE healthcare, Germany). Two flow cells of the CMD 50 d SPR sensorchip (Xantec Bioanalytics, Germany) were activated as previously described [21]. Each flow cell was then coated with Rho-1D4 as the primary antibody for the working surface and IgG1 (Sigma, Germany) for a negative control surface, both at a concentration of 0.1mg/ml in 10mM sodium acetate buffer pH 5. Then the surfaces were inactivated using 1M ethanolamine (Sigma, Germany). Immobilization of the Rho-1D4 antibody yielded 250 resonance units (RU) corresponding to 1.7 fmol/mm^2 (surface saturation was calculated by the amount of antibody bound, knowing that 1000 RU are equivalent to 1ng/mm^2). $GalR_1$, in 50mM MES containing 1mM $CaCl_2$ at pH 6 (running buffer) was then injected and bound to the Rho-1D4 antibody coated surface until saturation was reached. Flow rate was set to 5 µl/min.

Heterodimerization assay. For 5-HT_{1A} injections, the same buffer as for $GalR_1$ injection was used. Increasing concentrations of 5-HT_{1A} (50, 100 and 200nM) were injected to the $GalR_1$ coated surface. Two rounds of surface regeneration with 0.5% SDS were performed, before coating again with $GalR_1$. These cycles of regeneration and repeated immobilization of $GalR_1$ were done between each 5-HT_{1A} injection. Control injections were performed on an IgG1-coated surface and control data was subtracted from the $GalR_1$/5-HT_{1A} binding curves. SPR results were further analyzed for kinetic parameters. Binding constants were calculated by nonlinear curve fitting of the sensorgrams using BIAevaluation software (GE Healthcare, Germany).

Zinc exposed heterodimerization assays. In this case, 5-HT_{1A} that was going to be injected had been previously incubated with 200µM $ZnCl_2$. Then, the injection was performed over $GalR_1$ saturated surface in the running buffer. The surface was regenerated between each experiment. Bulk refractive index changes, originated from changes in the running solution due to the presence of zinc, were subtracted in order to facilitate recognition of protein binding and dissociation steps.

Construction of an atomistic model of the 5-HT_{1A} receptor by homology modeling

A starting model of the human 5-HT_{1A} receptor was constructed by homology modeling using the 5-HT_{1B} receptor as a template (PDB ID 4IAR). The sequences of the two receptors were aligned, taking into account the conserved motifs found in all GPCRs, as well as the location of the disulfide bridges.

These motifs, together with salt bridges, are important factors in constraining the conformation of the extracellular and transmembrane domains of the 5-HT_{1A} receptor. From the aligned sequences, a starting model of the receptor was constructed using the Modeller 9 version 8 (9v8) software [22]. Model validation was carried out using the MOE program (Chemical Computing Group Inc, Canada). In a subsequent step, the selective antagonist Rec 15/3079 was docked into the starting model using the GLIDE software [23]. Finally, the ligand-receptor complex was embedded in a lipid bilayer and refined using molecular dynamics. Specifically, the protein was embedded in a box consisting in a 1-palmitoyl-2-oleoyl-sn-glycero-3-phosphocholine (POPC) lipids and water molecules generated and equilibrated according to a previously described procedure [24]. The box had an initial size of 10.3 x 8.0 x 10.2nm^3 (XYZ), organized in such a way that the bilayer plane was oriented on the XY plane. Before protein insertion, the box contained 256 lipids (corresponding to an area per lipid of 0.64 nm^2) and circa 17000 water molecules. The protein was placed in the center of the box, and the overlapping molecules were removed. Particularly, all water molecules with oxygen atoms closer than 0.40nm to a non-hydrogen atom of the protein, as well as all lipid molecules with at least one atom closer than 0.25nm to a non-hydrogen atom of the protein, were removed. This resulted in a final system containing 197 lipids and circa 16000 water molecules. Next, 114 randomly selected water molecules were replaced by 58 sodium and 56 chloride ions, providing a neutral system with a concentration of approximately 0.2M NaCl. This concentration is fairly similar to that found in biological organisms, although they exhibit different intra and extracellular ion concentrations.

Sampling was carried out for 500ns using GROMACS package 4.6 [25]. From the simulations an average structure was generated and used for the identification of putative zinc binding sites. Accordingly, a zinc probe with the features of the zinc ion was passed through the model surface using the GRID22 (Molecular Discovery Ltd., UK) probe as implemented MOE program.

Results

Receptor expression and purification. Rho-1D4 tag was selected for purification due to three main reasons: small size, recognition by a very specific antibody and standardized purification method for rhodopsin, which belongs to the same GPCR family. Accordingly, 5-HT_{1A} and $GalR_1$ encoding genes were tagged with this Rho-1D4 immunogenic epitope for their purification. Moreover, the receptors were expressed in HEK293S GnTi$^-$ cells (lacking N-acetyl-glucosaminyltransferase activity) in order to

facilitate their electrophoretic analysis. Immunocytochemical staining of the tagged receptors clearly showed that the receptors were properly expressed and localized to the cell membrane (Fig. 1).

The rhodopsin standard immunopurification protocol was adapted and optimized for our receptors: triton X-100 was used instead of DM as solubilization detergent and MES was used as elution buffer (see Materials and Methods). The purified receptors were analyzed by Western blot and blue-native PAGE (Fig. 2). Western blot analysis revealed two bands for $GalR_1$ corresponding to pure monomeric (≈39 KDa) and dimeric forms (≈78 KDa), whereas 5-HT_{1A} showed only one band, corresponding to the monomer (≈46 KDa) (Fig. 2a). Under native conditions, in the blue-native PAGE gel, we obtained only monomeric bands for both proteins (Fig. 2b). Altogether, the electrophoretic results indicate that, under our purification conditions, the receptors are in a monomeric state for both receptors but in the case of $GalR_1$ a dimeric form could also be detected possibly due to the effect of the denaturing SDS agent.

Purified receptors folding state characterization by means of steady state fluorescence spectroscopy.

The presence of monomeric forms of the receptor under native conditions already suggested that the receptors were presumably in a native state but further proof was needed of correct folding of the receptors. To this aim we analyzed the Trp intrinsic steady state fluorescence of the purified receptors. Two parameters were carefully analyzed, the maximum emission wavelength and the fluorescence intensity. It is known that, under denaturing conditions, the protein maximum intensity band is red shifted and intensity decreases. These changes are caused by the fact that after protein unfolding Trp is located in a more hydrophilic environment, decreasing its quantum yield and in consequence the fluorescent intensity [26]. We used DTT and GdnHCl to detect receptor unfolding which should only be possible if the receptor is in a correctly folded state. $GalR_1$ has seven Trp (2% of total amino acid composition), and 5-HT_{1A} has the same number of Trp but in this case the proportion over total amino acid composition is lower (1.7%). In spite of this slight difference in Trp percentage, the two receptors behaved similarly under the two treatments used (Fig. 3). The starting maximum emission wavelength observed was slightly different for each receptor, 331nm for $GalR_1$ and 332nm 5-$HT_{1A,}$ because Trp residues are in different environments. In the two cases DTT treatment induced a 2nm red shift for both receptors, whereas no effect could be observed for L-Trp used as a control (Fig. S1, Supplementary material). However, in the case of $GalR_1$ the maximum shift was detected at lower DTT concentration, 4mM for $GalR_1$ and 6mM for 5-$HT_{1A,}$ as depicted in Fig. 3 (insets), where the maximum wavelength change regarding DTT concentration is represented. This would mean that 5-HT_{1A} is more stable under

our purification conditions, in agreement with the differences observed in the Western blot. Moreover, the two receptors eventually become completely denatured by GdnHCl and spectra typical for free Trp were obtained (Fig. S1, Supplementary material). The red shift and intensity decrease observed indicate that the two receptors are properly folded and this allows their use for the protein-protein interaction analysis carried out in this work.

G-Protein Activation. We have previously shown that the receptors could be purified in a folded state but it is important to know whether or not they are functional. The functionality of the receptors was measured by their ability to activate their specific G-proteins by means of a fluorescence spectroscopic assay. We used Gαi1 for $GalR_1$ and Gαi2 for 5-HT_{1A} activation, as it has been previously described that our target receptors are able to signal via these specific Gα subunits [27,28], when they are activated by their corresponding ligands. Here, adding 8-OH-DPAT for 5-HT_{1A} or galanin (1-29) peptide for $GalR_1$ was not necessary because the receptors have been already purified bound to their ligands during the purification process. In this study we monitored intrinsic fluorescence changes of a highly conserved Trp in Gα proteins, which fluorescence increases as a result of the conformational change induced in the subunit by the receptor upon binding and activation. We could detect activity of the receptors in both cases as indicated by the typical saturation fluorescence curve obtained after GTPγS addition (Fig. 4) [29].

Zinc effect on 5-HT_{1A}- $GalR_1$ heterodimerization. Once we showed that the receptors can be purified in a functionally active state, we carried out a detailed characterization of the heterodimerization process between them, and the effect of zinc on the process. We used SPR spectroscopy as the analytical technique to follow the interaction between the two receptors receptors due to its capacity of studying the molecular recognition event very specifically in a real time manner. In a first step, we checked if we were able to detect heterodimerization by SPR. As the receptors were tagged with the Rho-1D4 immunogenic epitope, the corresponding Rho-1D4 antibody was immobilized onto the chip surface. Then $GalR_1$ was injected until surface saturation was achieved by reaching 1.1-2.2fmol $GalR_1$ per mm^2, and finally 5-HT_{1A} was injected into the running buffer at different concentrations (50, 100 and 200nM). When the binding experiment was concluded, 0.5% SDS was applied to regenerate the surface between each 5-HT_{1A} injection. Since regeneration could also remove $GalR_1$ from the surface, the surface was saturated again with this receptor before a new sample of 5-HT_{1A} was injected. Our results showed a clear interaction between the receptors and the SPR response amplitude increased as a

function of the injected concentration of 5-HT_{1A} (Fig. 5). A global fit analysis of sensorgrams revealed nearly identical values for the association rate constants averaging at $1.09\times10^{4}M^{-1}s^{-1}$ (Fig. 5a). However, the heterodimer protein complex remained stably bound, when running buffer was flushed over the chip surface as shown in the sensorgrams (Fig. 5a). The dissociation phase was fit separately for each curve yielding values between $1\times10^{-5}s^{-1}$ and $8\times10^{-5}s^{-1}$, and the resulting K_D values were 0.9 and 7nM.

The next step was to investigate the effect of zinc on the observed heterodimerization. For this experiment, the 5-HT_{1A} sample to be injected was previously treated with 200μM $ZnCl_2$. 5-HT_{1A} ability to bind $GalR_1$ was completely abolished in the $ZnCl_2$ containing sample, as observed by the different binding signals with respect to amplitude and kinetics (Fig. 5b). Although a certain degree of binding can be detected, the protein complex dissociated completely, when running buffer was flushed over the sensorchip. We attribute the positive SPR signal to unspecific binding of 5-HT_{1A} to the sensorchip, since the negative control curve (experimental replicate over a surface coated with IgG1) exhibited the same curve characteristics including the fast dissociation phase that went below the zero baseline (compare Fig. 5b with Fig. S2, Supplementary material).

In order to provide further evidence that would confirm our SPR results we used a complementary approach. We carried out FRET analysis of the process because this is one of the most established technologies to study GPCR heterodimerization, and also because the 5-HT_{1A}-$GalR_1$ heteromer was first detected using this method [6]. We used standardized protocols for this purposes that should validate the reliability of our results. With this purpose 5-HT_{1A} and $GalR_1$ receptors were tagged with ECFP (excitation at 410nm and emission at 480nm) and EYFP (excitation: 517nm and emission 525nm) respectively and transient transfection was carried out by adding $ZnCl_2$ in the transfection media at the indicated concentrations mentioned (see Materials and Methods). The same experiment was performed with ECFP-EYFP fusion protein as negative control (Fig. S3, Supplementary material).

For our receptors, under physiological conditions, the presence of FRET could be clearly observed (Fig. 6, continous trace). EYFP band is present when excitation is set at 410nm (ECFP excitation wavelength), whereas the ECFP band (compared to the expressed protein alone band) is smaller due to the energy transfer from ECFP to EYFP. After zinc exposure, at a concentration of 50μM $ZnCl_2$, the FRET signal was significantly diminished (there is an increment of ECFP emission and a concomitant decrease in EYFP emission) (Fig. 6, dashed trace). The results clearly show that zinc affects the

fluorescent energy transfer between the two fluorescent proteins tagged to the receptors. Higher zinc concentrations caused only minor changes. The FRET and SPR results taken together confirm our initial hypothesis that zinc antagonizes heteromer formation between $GalR_1$ and 5-HT_{1A}.

Identification of putative binding sites of Zn on the 5-HT_{1A} receptor

Based on previous results [30], it appeared that zinc could directly interact with the 5-HT_{1A} receptor. Our FRET and SPR results suggest such an interaction and that the interaction sites could match with heterodimerization sites. So, molecular modeling was applied in order to get further insights into this question. The results of this calculation are shown pictorially in Fig. 7 where the spheres represent favorable sites for zinc binding. Most of the putative binding sites are located on the extracellular and intracellular loops, although a few of them are located on the transmembrane regions including TM1, and the TM4 -TM5 and TM6-TM7 interfaces.

Discussion

Homo- and heterodimerization have emerged as a very important mechanism for regulating GPCRs function and signaling [31]. Unbalancing these receptor-receptor interactions can have physiological consequences and play a role in the physiopathogenesis of a number of diseases. In the case of the receptors we have studied, it was recently reported that the 5-HT_{1A} and $GalR_1$ receptors could heterodimerize and that this interaction could be relevant in the molecular mechanism of depression [6]. . We decided to get a deeper insight into this interaction by studying in detail the process in a purified system. Furthermore, we hypothesized that zinc could affect this interaction and we have analyzed the effect of this ion on the heterodimerization process. We based our hypothesis on the fact that zinc plays an important role in many biological processes [32], especially in those involved in mental disorders as we are going to discuss further.

We have purified the two receptors by using a strategy that has been proven useful for other GPCRs [33]. This approach consisted in adding the Rho-1D4 tag (the epitope corresponding to the last 9 amino acids of rhodopsin) at the C-terminal tail of the receptor and using triton X-100 as solubilizing agent. In addition we have used HEK293S GnTi$^-$ cell line for expression of the recombinant receptors. This cell line abolishes protein glycosylation facilitating analysis by electrophoretic methods. This strategy has

allowed efficient expression and purification of the receptors -for characterization purposes- without changing, in principle, the native protein expression and cellular localization. Our preliminary purification efforts resulted in aggregated receptors that did not show functional activity (data not shown), we solved this problem by purifying the receptors in the presence of their ligand, that had been successfully used in the purification of other receptors [34,35]. In this case we were able to obtain purified receptors that did not appear to be aggregated judged from the UV spectra and electrophoretic pattern. The blue native gel indicated that both receptors were purified in a monomeric state. In turn, our Western blot (from SDS-PAGE gel) analysis showed what appeared to be a dimeric band in the case of the $GalR_1$ that was not apparent in the blue native gel. This may seem contradictory but we should take into account that SDS can induce artifactual oligomerization [36]. The electrophoretic pattern, however, did not assure that the protein was correctly folded. This was verified by means of both Trp intrinsic fluorescence measurements and immunocytochemical localization. Trp intrinsic fluorescence had already been used for this purpose [37]. We found that after DTT treatment, the fluorescence maximum emission band underwent a shift reflecting a change in the Trp environment compatible with a partial loss of protein structure (Fig. 3). Moreover, after GdnHCl exposure, our receptor spectra shape changed to that of free L-Trp one, indicating that the protein had been completely denatured. A difference was detected in the denaturing pattern derived from these experiments for $5\text{-}HT_{1A}$ and $GalR_1$. This was the shift observed at higher DTT concentrations for $5HT_{1A}$ receptor and this could be interpreted as this receptor being more resistant to partial unfolding than $GalR_1$. Immunocytochemical analysis showed that the two receptors were expressed at the cell membrane (and not retained in the endoplasmic reticulum) (Fig.1) reinforcing that the purified receptors were correctly folded under our experimental conditions. A final proof of the native status of the purified receptors was obtained from determining its G-protein activation capacity. In both cases we were able to detect G-protein activation by means of a fluorescence assay after GTPγS addition (Fig. 4) proving that the receptors had been purified in a functional state although the slightly different activation patterns observed could reflect subtle differences in activation kinetics. This, together with the Trp fluorescence results suggest, that the purified receptors have slightly different functional conformations in the purified state, caused either by the intrinsic characteristics of each receptor or by the purification conditions. Nevertheless, this does not represent any problem in our subsequent interaction analysis.

The purification of the two receptors was successfully completed and this allowed us to investigate the heterodimerization process in real time by means of SPR spectroscopy that has been shown to be appropriate for studying protein-protein interactions [38]. We have been able to successfully characterize the rhodopsin activation process by means of this technique [21]. In spite of the many advantages of this technique like high sensitivity and reliability, its application to GPCR analysis is still under development [39]. Furthermore, no previous study involving our receptors has been reported and this highlights the novelty of our approach. Our SPR measurements clearly showed that $5HT_{1A}$ and $GalR_1$ heterodimerize in the purified state and that this interaction is stable under our experimental conditions (Fig. 5). We derived an association rate constant (Ka) of $1.09\times10^{4}M^{-1}\times s^{-1}$ and by taking the highest and lowest dissociation rate constants (Kd, see above in Results section), we end up with dissociation constants K_D between 0.9 and 7nM indicating a tight and stable complex formation. Rate and affinity constants for this dimerization process are of similar magnitude as the rhodopsin-transducin interaction investigated by the same methodological SPR approach [40].

One of the important goals of our study was to test the effect of zinc on the heterodimerization process between our receptors. Zinc is a widespread metal ion involved in many physiological processes and found in all body tissues including the eye, brain and others. Zinc deficiency can result in unhealthy state and be the cause of certain pathological states like depression [41,42]. We have previously shown a clear effect of zinc on the structure and stability of visual rhodopsin [43] and other examples involving zinc and GPCRs could be found [44,45]. Zinc has also been shown to interact with other GPCRs, including its cognate receptor GPR39 [46] and $5\text{-}HT_{1A}$ where it has been proposed to act as an allosteric modulator of the serotonin receptor function [30]. We find that zinc impairs $5\text{-}HT_{1A}$-$GalR_1$ heterodimerization. When we exposed $5\text{-}HT_{1A}$ receptor to $ZnCl_2$ and injected it over $GalR_1$, immobilized on the SPR sensorchip, we could detect relative low levels of receptor binding, compared with control sample in the absence of zinc (Fig. 5a and 5b), that could be removed upon washing with buffer. This lower level of binding and the complete removal of the receptor after washing would indicate a transient interaction much less stable than the one observed in the absence of zinc. The described data suggests that the presence of zinc impairs heterodimerization of the two receptors. We also analyzed the effect of zinc by means of FRET on cells expressing the receptors in order to further validate the results obtained in the purified system. We observed, in HEK293T cells, a clear decrease in FRET intensity in the presence of zinc consistent with heterodimer formation impairment (Fig. 6).

The FRET measurements in cells are in agreement with the SPR measurements obtained with purified receptors. According to the SPR analysis, zinc impaired heterodimer formation completely but under *in vivo* conditions, in the FRET measurements, we cannot discard that some heterodimerization was still present at 50μM $ZnCl_2$, due to the presence of the ECFP second emission band that could mask EYFP less intense signals, but we can clearly see a significant decrease in the FRET signal at 50μM $ZnCl_2$. A meta-analysis study performed in 1643 depressed patients and 804 controls revealed that the average zinc blood concentration was 13.31μM and 15.18μM respectively [47]. Other studies describe that the zinc concentration increases significantly in the synaptic environment and, based on experimental results, they suggest 50μM as a physiological relevant zinc concentration [30]. Therefore, the zinc concentration used in our FRET experiments are in agreement with the reported physiological concentration for zinc. The difference between the FRET and SPR data could result from additional zinc binding components that are present in living cells, but not in the controlled environment of the SPR experiments. However, higher concentrations of $ZnCl_2$ did not significantly alter the FRET signal suggesting the existence of mechanisms that may counterbalance the zinc concentration increment effect in the cell environment. Alternatively, it is possible that in cells, 50μM $ZnCl_2$, completely abolished heterodimer formation and this would indicate that the SPR results reveal the intrinsic features of the receptors because in this case we are analyzing them in their purified state.

Concerning the mechanism by which zinc ions prevent heterodimer formation, one possible explanation is that zinc acts as a protein-protein interaction inhibitor by binding to a site located on the interface surface impairing dimerization. In spite of the fact that the interacting interface of the 5-HT_{1A}-$GalR_1$ heterodimer has yet to be identified, our present modeling results confirm that the putative zinc-binding sites at TM1, and the TM4-TM5 and TM6-TM7 interfaces (Fig. 7) may be located on the putative oligomerization interfaces found in the analysis of the diverse GPCR crystallographic structures available: either TM1-TM2-H8 or TM5, sometimes together with TM4 and others with TM6, also involving the ICL2 intracellular loop [48,49]. Moreover, previous reports suggest the specific involvement of TM4 and TM5 in such an interaction [4]. These results provide support to a specific role of zinc as an inhibitor of protein-protein interactions but further studies, like mutagenesis of specific amino acids, should be carried out in order to fully describe the specific details of the Zn-5-HT_{1A}-$GalR_1$ interactions.

In conclusion, here we have described an effect of zinc on the $GalR_1$-5-HT_{1A} heterodimer formation. Our results fit nicely with the antidepressive effects that had been widely described for zinc, and validate our hypothesis that the presence of the metal ion can be important in modulating the balance between monomers/heterodimers of the receptors studied and that this may play a significant role in the development of major depressive disorder. Our findings suggest that zinc is a modulator of the specific heterodimerization between 5-HT_{1A}-$GalR_1$ and that zinc homeostasis can play a critical role in this interaction. Thus, in a given environment with appropriate zinc concentration, the receptors would be present mostly in their monomeric form, with only a small fraction of heteromers, and that would correspond to a healthy state. Upon zinc levels decrease, the heteromer fraction could possibly increase giving rise to a disease phenotype (Fig. 8).

Our results reinforce the notion of 5-HT_{1A}-$GalR_1$ heterodimer as one of the underlying molecular causes of the depressive phenotype, and provide a rationale for the zinc clinical effects that have been previously reported. Additionally, having the receptors in a purified active state provides new opportunities for structural determination by appropriate techniques, such as X-ray crystallography.

Acknowledgements

We thank Dr. Dasiel Borroto-Escuela for providing pECFP-5-HT_{1A} and pEYFP-$GalR_1$ constructs. This work has been supported by grants from Fundació la Marató de TV3 (090131-01) and AGAUR (2009 SGR 1402) to PG. MT is the recipient of a predoctoral fellowship FPI-UPC from Universitat Politècnica de Catalunya.

Conflict of Interest: The authors declare that they have no conflict of interest.

References

1. Nichols DE, Nichols CD (2008) Serotonin receptors. Chemical reviews 108 (5):1614-1641. doi:10.1021/cr078224o
2. Hannon J, Hoyer D (2008) Molecular biology of 5-HT receptors. Behavioural brain research 195 (1):198-213. doi:10.1016/j.bbr.2008.03.020
3. Lesch KP (1991) 5-HT1A receptor responsivity in anxiety disorders and depression. Progress in neuro-psychopharmacology & biological psychiatry 15 (6):723-733
4. Gorinski N, Kowalsman N, Renner U, Wirth A, Reinartz MT, Seifert R, Zeug A, Ponimaskin E, Niv MY (2012) Computational and experimental analysis of the transmembrane domain 4/5 dimerization interface of the serotonin 5-HT(1A) receptor. Molecular pharmacology 82 (3):448-463. doi:10.1124/mol.112.079137
5. Cussac D, Rauly-Lestienne I, Heusler P, Finana F, Cathala C, Bernois S, De Vries L (2012) mu-Opioid and 5-HT1A receptors heterodimerize and show signalling crosstalk via G protein and MAP-kinase pathways. Cellular signalling 24 (8):1648-1657. doi:10.1016/j.cellsig.2012.04.010
6. Borroto-Escuela DO, Narvaez M, Marcellino D, Parrado C, Narvaez JA, Tarakanov AO, Agnati LF, Diaz-Cabiale Z, Fuxe K (2010) Galanin receptor-1 modulates 5-hydroxtryptamine-1A signaling via heterodimerization. Biochemical and biophysical research communications 393 (4):767-772. doi:10.1016/j.bbrc.2010.02.078
7. Branchek T, Smith KE, Walker MW (1998) Molecular biology and pharmacology of galanin receptors. Annals of the New York Academy of Sciences 863:94-107
8. Lori A, Tang Y, O'Malley S, Picciotto MR, Wu R, Conneely KN, Cubells JF (2011) The galanin receptor 1 gene associates with tobacco craving in smokers seeking cessation treatment. Neuropsychopharmacology : official publication of the American College of Neuropsychopharmacology 36 (7):1412-1420. doi:10.1038/npp.2011.25
9. Gold AB, Wileyto EP, Lori A, Conti D, Cubells JF, Lerman C (2012) Pharmacogenetic association of the galanin receptor (GALR1) SNP rs2717162 with smoking cessation. Neuropsychopharmacology : official publication of the American College of Neuropsychopharmacology 37 (7):1683-1688. doi:10.1038/npp.2012.13
10. Mazarati A, Lu X (2005) Regulation of limbic status epilepticus by hippocampal galanin type 1 and type 2 receptors. Neuropeptides 39 (3):277-280. doi:10.1016/j.npep.2004.12.003

11. Misawa K, Ueda Y, Kanazawa T, Misawa Y, Jang I, Brenner JC, Ogawa T, Takebayashi S, Grenman RA, Herman JG, Mineta H, Carey TE (2008) Epigenetic inactivation of galanin receptor 1 in head and neck cancer. Clinical cancer research : an official journal of the American Association for Cancer Research 14 (23):7604-7613. doi:10.1158/1078-0432.CCR-07-4673

12. Fuxe K, Marcellino D, Rivera A, Diaz-Cabiale Z, Filip M, Gago B, Roberts DC, Langel U, Genedani S, Ferraro L, de la Calle A, Narvaez J, Tanganelli S, Woods A, Agnati LF (2008) Receptor-receptor interactions within receptor mosaics. Impact on neuropsychopharmacology. Brain research reviews 58 (2):415-452. doi:10.1016/j.brainresrev.2007.11.007

13. Fuxe K, Ogren SO, Jansson A, Cintra A, Harfstrand A, Agnati LF (1988) Intraventricular injections of galanin reduces 5-HT metabolism in the ventral limbic cortex, the hippocampal formation and the fronto-parietal cortex of the male rat. Acta physiologica Scandinavica 133 (4):579-581. doi:10.1111/j.1748-1716.1988.tb08444.x

14. Nowak G, Sowa-Kucma M, Szewczyk B, Poleszak E, Pilc A (2010) Zinc and magnesium interaction with glutamate system in depression. Pharmacological Reports 62:23-23

15. Siwek M, Dudek D, Paul IA, Sowa-Kucma M, Zieba A, Popik P, Pilc A, Nowak G (2009) Zinc supplementation augments efficacy of imipramine in treatment resistant patients: a double blind, placebo-controlled study. Journal of affective disorders 118 (1-3):187-195. doi:10.1016/j.jad.2009.02.014

16. Nowak G, Siwek M, Dudek D, Zieba A, Pilc A (2003) Effect of zinc supplementation on antidepressant therapy in unipolar depression: a preliminary placebo-controlled study. Polish journal of pharmacology 55 (6):1143-1147

17. Holst B, Egerod KL, Schild E, Vickers SP, Cheetham S, Gerlach LO, Storjohann L, Stidsen CE, Jones R, Beck-Sickinger AG, Schwartz TW (2007) GPR39 signaling is stimulated by zinc ions but not by obestatin. Endocrinology 148 (1):13-20. doi:10.1210/en.2006-0933

18. Mlyniec K, Budziszewska B, Reczynski W, Sowa-Kucma M, Nowak G (2013) The role of the GPR39 receptor in zinc deficient-animal model of depression. Behavioural brain research 238:30-35. doi:10.1016/j.bbr.2012.10.020

19. Toledo D, Ramon E, Aguila M, Cordomi A, Perez JJ, Mendes HF, Cheetham ME, Garriga P (2011) Molecular mechanisms of disease for mutations at Gly-90 in rhodopsin. J Biol Chem 286 (46):39993-40001. doi:10.1074/jbc.M110.201517

20. Srinivasan S, Je SH, Back S, Barin G, Buyukcakir O, Guliyev R, Jung Y, Coskun A (2014) Ordered Supramolecular Gels Based on Graphene Oxide and Tetracationic Cyclophanes. Adv Mater 26 (17):2725-2729. doi:Doi 10.1002/Adma.201304334

21. Komolov KE, Aguila M, Toledo D, Manyosa J, Garriga P, Koch KW (2010) On-chip photoactivation of heterologously expressed rhodopsin allows kinetic analysis of G-protein signaling by surface plasmon resonance spectroscopy. Analytical and bioanalytical chemistry 397 (7):2967-2976. doi:10.1007/s00216-010-3876-4

22. Sali A, Blundell TL (1993) Comparative protein modelling by satisfaction of spatial restraints. Journal of molecular biology 234 (3):779-815. doi:10.1006/jmbi.1993.1626

23. Friesner RA, Banks JL, Murphy RB, Halgren TA, Klicic JJ, Mainz DT, Repasky MP, Knoll EH, Shelley M, Perry JK, Shaw DE, Francis P, Shenkin PS (2004) Glide: a new approach for rapid, accurate docking and scoring. 1. Method and assessment of docking accuracy. Journal of medicinal chemistry 47 (7):1739-1749. doi:10.1021/jm0306430

24. Cordomi A, Perez JJ (2007) Molecular dynamics simulations of rhodopsin in different one-component lipid bilayers. The journal of physical chemistry B 111 (25):7052-7063. doi:10.1021/jp0707788

25. Van Der Spoel D, Lindahl E, Hess B, Groenhof G, Mark AE, Berendsen HJ (2005) GROMACS: fast, flexible, and free. Journal of computational chemistry 26 (16):1701-1718. doi:10.1002/jcc.20291

26. Eftink MR (1994) The use of fluorescence methods to monitor unfolding transitions in proteins. Biophys J 66 (2 Pt 1):482-501

27. Gillison SL, Sharp GW (1994) ADP ribosylation by cholera toxin identifies three G-proteins that are activated by the galanin receptor. Studies with RINm5F cell membranes. Diabetes 43 (1):24-32

28. Talbot JN, Jutkiewicz EM, Graves SM, Clemans CF, Nicol MR, Mortensen RM, Huang X, Neubig RR, Traynor JR (2010) RGS inhibition at G(alpha)i2 selectively potentiates 5-HT1A-mediated antidepressant effects. Proceedings of the National Academy of Sciences of the United States of America 107 (24):11086-11091. doi:10.1073/pnas.1000003107

29. Farrens DL, Altenbach C, Yang K, Hubbell WL, Khorana HG (1996) Requirement of rigid-body motion of transmembrane helices for light activation of rhodopsin. Science 274 (5288):768-770

30. Barrondo S, Salles J (2009) Allosteric modulation of 5-HT(1A) receptors by zinc: Binding studies. Neuropharmacology 56 (2):455-462. doi:10.1016/j.neuropharm.2008.09.018

31. Tena-Campos M, Ramon E, Rivera D, Borroto-Escuela DO, Romero-Fernandez W, Fuxe K, Garriga P (2014) G-protein-coupled receptors oligomerization: emerging signaling units and new opportunities for drug design. Current protein & peptide science 15 (7):648-658

32. Frassinetti S, Bronzetti G, Caltavuturo L, Cini M, Croce CD (2006) The role of zinc in life: a review. Journal of environmental pathology, toxicology and oncology : official organ of the International Society for Environmental Toxicology and Cancer 25 (3):597-610

33. Wong JP, Reboul E, Molday RS, Kast J (2009) A carboxy-terminal affinity tag for the purification and mass spectrometric characterization of integral membrane proteins. Journal of proteome research 8 (5):2388-2396. doi:10.1021/pr801008c

34. Corin K, Baaske P, Geissler S, Wienken CJ, Duhr S, Braun D, Zhang S (2011) Structure and function analyses of the purified GPCR human vomeronasal type 1 receptor 1. Scientific reports 1:172. doi:10.1038/srep00172

35. Fay JF, Farrens DL (2012) A key agonist-induced conformational change in the cannabinoid receptor CB1 is blocked by the allosteric ligand Org 27569. The Journal of biological chemistry 287 (40):33873-33882. doi:10.1074/jbc.M112.352328

36. Watt AD, Perez KA, Rembach A, Sherrat NA, Hung LW, Johanssen T, McLean CA, Kok WM, Hutton CA, Fodero-Tavoletti M, Masters CL, Villemagne VL, Barnham KJ (2013) Oligomers, fact or artefact? SDS-PAGE induces dimerization of beta-amyloid in human brain samples. Acta neuropathologica 125 (4):549-564. doi:10.1007/s00401-013-1083-z

37. Lin S, Gether U, Kobilka BK (1996) Ligand stabilization of the beta 2 adrenergic receptor: effect of DTT on receptor conformation monitored by circular dichroism and fluorescence spectroscopy. Biochemistry-Us 35 (46):14445-14451. doi:10.1021/bi961619+

38. Leonard P, Hearty S, O'Kennedy R (2011) Measuring protein-protein interactions using Biacore. Methods in molecular biology 681:403-418. doi:10.1007/978-1-60761-913-0_22

39. Locatelli-Hoops S, Yeliseev AA, Gawrisch K, Gorshkova I (2013) Surface plasmon resonance applied to G protein-coupled receptors. Biomedical spectroscopy and imaging 2 (3):155-181. doi:10.3233/BSI-130045

40. Komolov KE, Senin, II, Philippov PP, Koch KW (2006) Surface plasmon resonance study of g protein/receptor coupling in a lipid bilayer-free system. Analytical chemistry 78 (4):1228-1234. doi:10.1021/ac051629t

41. Prasad AS (2014) Impact of the discovery of human zinc deficiency on health. Journal of trace elements in medicine and biology : organ of the Society for Minerals and Trace Elements. doi:10.1016/j.jtemb.2014.09.002

42. Jurowski K, Szewczyk B, Nowak G, Piekoszewski W (2014) Biological consequences of zinc deficiency in the pathomechanisms of selected diseases. Journal of biological inorganic chemistry : JBIC : a publication of the Society of Biological Inorganic Chemistry 19 (7):1069-1079. doi:10.1007/s00775-014-1139-0

43. del Valle LJ, Ramon E, Canavate X, Dias P, Garriga P (2003) Zinc-induced decrease of the thermal stability and regeneration of rhodopsin. The Journal of biological chemistry 278 (7):4719-4724. doi:10.1074/jbc.M210760200

44. Muller A, Kleinau G, Piechowski CL, Muller TD, Finan B, Pratzka J, Gruters A, Krude H, Tschop M, Biebermann H (2013) G-protein coupled receptor 83 (GPR83) signaling determined by constitutive and zinc(II)-induced activity. PloS one 8 (1):e53347. doi:10.1371/journal.pone.0053347

45. Hojyo S, Fukada T, Shimoda S, Ohashi W, Bin BH, Koseki H, Hirano T (2011) The zinc transporter SLC39A14/ZIP14 controls G-protein coupled receptor-mediated signaling required for systemic growth. PloS one 6 (3):e18059. doi:10.1371/journal.pone.0018059

46. Popovics P, Stewart AJ (2011) GPR39: a Zn(2+)-activated G protein-coupled receptor that regulates pancreatic, gastrointestinal and neuronal functions. Cell Mol Life Sci 68 (1):85-95. doi:10.1007/s00018-010-0517-1

47. Swardfager W, Herrmann N, Mazereeuw G, Goldberger K, Harimoto T, Lanctot KL (2013) Zinc in depression: a meta-analysis. Biol Psychiatry 74 (12):872-878. doi:10.1016/j.biopsych.2013.05.008

48. Manglik A, Kruse AC, Kobilka TS, Thian FS, Mathiesen JM, Sunahara RK, Pardo L, Weis WI, Kobilka BK, Granier S (2012) Crystal structure of the micro-opioid receptor bound to a morphinan antagonist. Nature 485 (7398):321-326. doi:10.1038/nature10954

49. Huang J, Chen S, Zhang JJ, Huang XY (2013) Crystal structure of oligomeric beta1-adrenergic G protein-coupled receptors in ligand-free basal state. Nature structural & molecular biology 20 (4):419-425. doi:10.1038/nsmb.2504

Figure legends

Fig. 1 *Expression and cellular localization of 5-HT$_{1A}$ and GalR$_1$*. HEK 293S GnTi$^-$ cells, transiently transfected with the receptor genes were fixed, immunostained with FITC (see Materials and Methods) and analyzed by fluorescence microscopy. 5-HT$_{1A}$ (a-c) and GalR$_1$ (d-f) receptors are shown in green and nuclei stained with DAPI, in blue.

Fig. 2 *Electrophoretic analysis of the expressed purified recombinant receptors.* (a) Western-Blot. Samples were loaded onto a SDS-PAGE gel and upon transferring onto a nitrocellulose membrane, receptors were immunodetected. Loading order from left to right was as follows: GalR$_1$ and 5-HT$_{1A}$. Bands reveal the presence of our specific proteins but also the presence of species with higher apparent molecular weight for GalR$_1$ protein. (b) Blue-native PAGE. Samples in 50mM MES buffer, 5% glycerol and 0.04% Ponceau (final concentrations) were loaded according to the following order from left to right: molecular weight marker (MW), BSA, GalR$_1$ and 5-HT$_{1A}$. Double marker was used to confirm ladder band weight, because of the variations of native marker migration in different native gels. The gel reveals that the receptors are purified as monomers. The position of the molecular weight protein marker is indicated on the left in kDa.

Fig. 3 *Chemical unfolding of the purified receptors*. Effect of DTT and GdnHCl on the maximum emission wavelength (λmax) of purified GalR$_1$ (a) and 5-HT$_{1A}$ receptor (b). The different conditions are native protein (—), 10mM DTT exposure (----) and 10mM DTT and 6M GdnHCl exposure (···). The proteins (1μM) were treated with 10mM DTT and 6M GdnHCl during 30min at RT. For GalR$_1$, DTT induces a λmax red shift from 331nm to 333nm and GdnHCl together with DTT induces λmax a shift to 352nm, giving a similar shape to the free Trp solution spectra. For 5-HT$_{1A}$, DTT induces λmax red shift from 332nm to 334nm and GdnHCl together with DTT induces λmax a shift to 352nm as in GalR$_1$. *Inset.* Dose response of the DTT induced λmax shift for both receptors. Purified proteins were exposed to DTT using the following concentrations (0, 1.5, 3, 4.5, 6 and 10mM) during 15 min for each concentration. Δλmax was determined from the difference between the λmax of DTT treated samples and control. Curves correspond to the average of three independent experiments

Fig. 4 *G-protein activation of the purified receptors***.** GTPγS binding to the G protein upon receptor activation was detected by means of a fluorescence assay. Time-based emission scans for Gαi1 activation by $GalR_1$ (a) and Gαi2 by 5-HT_{1A} (b) are presented. In both cases we can see a curve showing the three typical phases of an activation experiment [29]: baseline, GTPγS binding and saturation phase or plateau, concluding that, under our specific purification conditions we obtained active proteins. Curves correspond to the average of three independent experiments

Fig. 5 *SPR analysis of 5-HT_{1A}-$GalR_1$ dimerization in the presence and absence of zinc.* (a) Specific heterodimerization between the two purified receptors. Data show a direct relationship between the concentration of 5-HT_{1A} injected -onto a $GalR_1$ coated sensorchip- and the amount of receptor bound. Response curves for $GalR_1$ binding upon 200nM 5-HT_{1A} injection (Ka = 1.04 x$10^4M^{-1}s^{-1}$) (—), 100nM (Ka = 1.07 x$10^4M^{-1}s^{-1}$) (----) and 50nM (Ka = 1.17 x$10^4M^{-1}s^{-1}$) injection (···). SPR curves show clearly the interaction between the two receptors with an average association rate constant (Ka) of 1.09x$10^4M^{-1}s^{-1}$ (Ka was calculated after subtraction of the negative control to each sample). It is interesting to highlight that nearly no dissociation can be detected. (b) Effect of $ZnCl_2$ exposure on 5-HT_{1A}- $GalR_1$ heteromer by SPR. Response curve shows no binding of $GalR_1$ after 5-HT_{1A}-$ZnCl_2$ mixture injection. Although there is a small binding response, it dissociates completely

Fig. 6 *In vivo heterodimerization analyzed by FRET spectroscopy*. Effect of $ZnCl_2$ exposure on 5-HT_{1A}- $GalR_1$ heteromer by FRET. Fluorescent spectra show a decrease in the FRET signal, suggesting heterodimer dissociation, after 50μM (----) $ZnCl_2$ exposure compared to non-exposed receptors (—). At higher concentrations, such as 100μM (···) and 200μM. no further increase can be detected when compared to the 50 μM $ZnCl_2$ sample. Arrows show differences in fluorescence intensity upon zinc addition.

Fig. 7 *Zinc binding sites determined by molecular modeling*. Ribbon representation of the constructed $5HT_{1A}$ receptor model (blue) resulting from our present studies. Spheres in green represent the binding sites of the zinc ion computed using a specific probe

Fig. 8 *Scheme of zinc inhibition of heterodimer formation***.** The effect of zinc on 5-HT_{1A}-$GalR_1$ heterodimer formation is summarized. Under physiological zinc deficient conditions, the heterodimer would be the predominant form, causing a disease phenotype. In the presence of high zinc concentration, the metal ion can interact with the receptor (in our case we propose with 5-HT_{1A}), impairing dimer formation and this would reflect a healthy phenotype

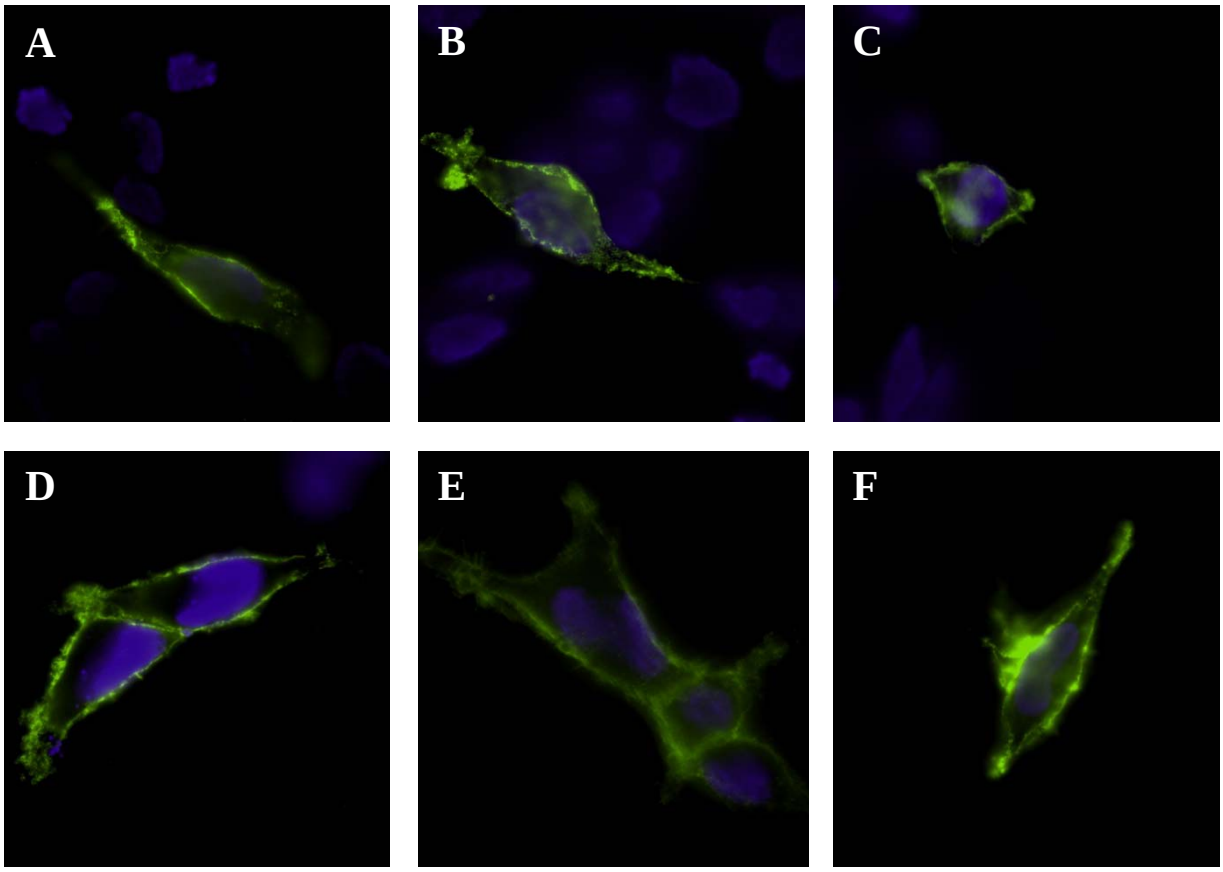

Figure 1

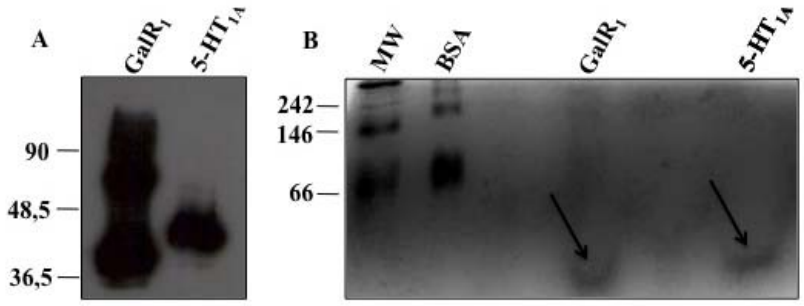

Figure 2

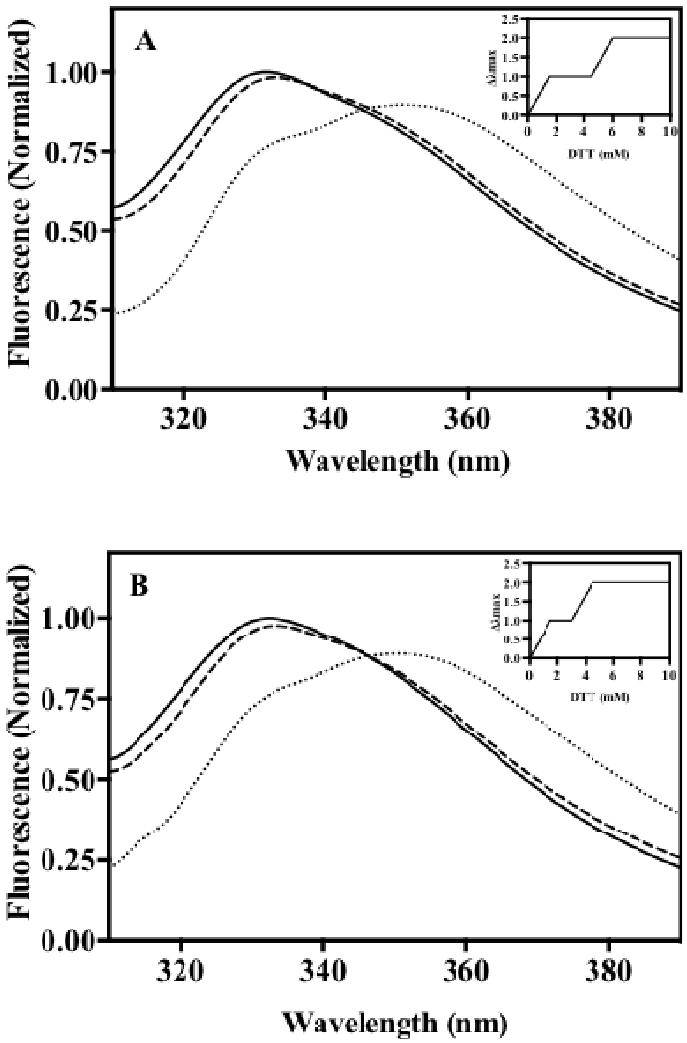

Figure 3

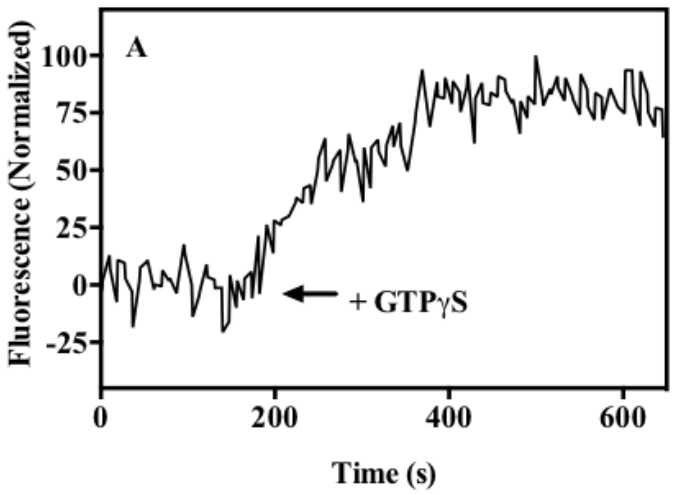
A
Fluorescence (Normalized)
100
75
50
25
0
-25
+ GTPγS
0
200
400
600
Time (s)

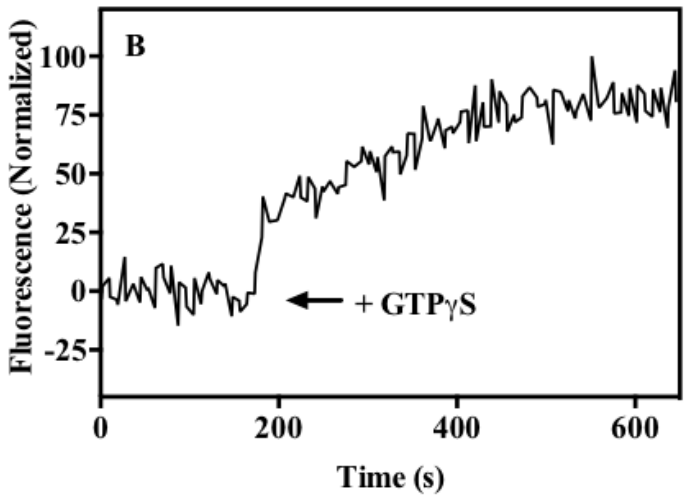
B
Fluorescence (Normalized)
100
75
50
25
0
-25
+ GTPγS
0
200
400
600
Time (s)

Figure 4

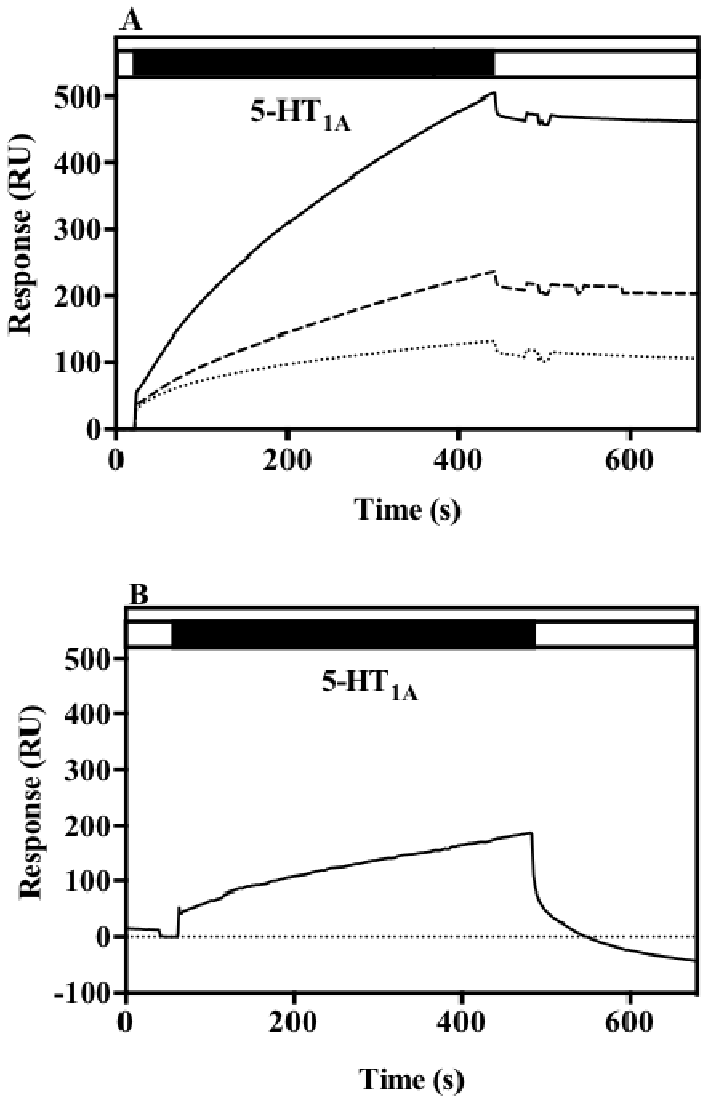
A
5-HT1A
Response (RU)
500
400
300
200
100
0
0
200
400
600
Time (s)
B
5-HT1A
Response (RU)
500
400
300
200
100
0
-100
0
200
400
600
Time (s)

Figure 5

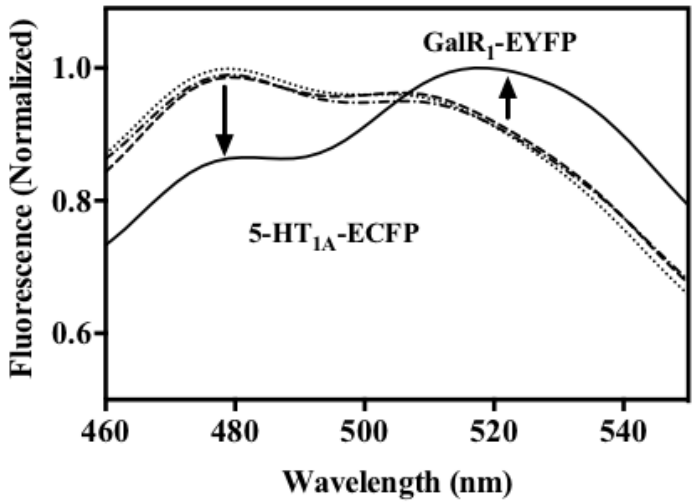
Fluorescence (Normalized)
1.0
0.8
0.6
460
480
500
520
540
Wavelength (nm)
GalR1-EYFP
5-HT1A-ECFP

Figure 6

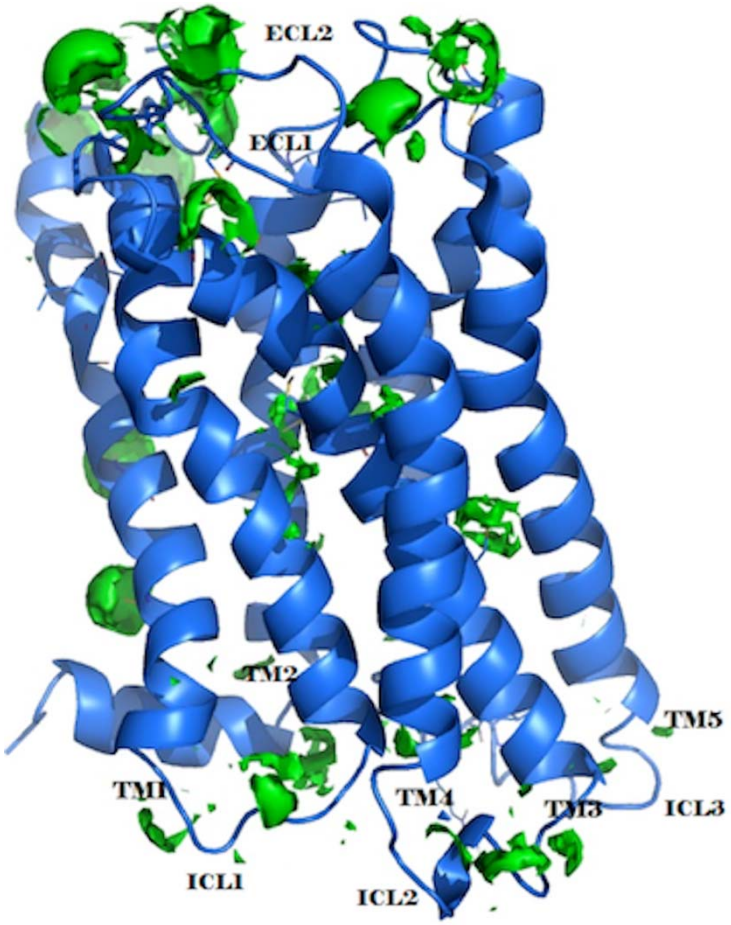

Figure 7

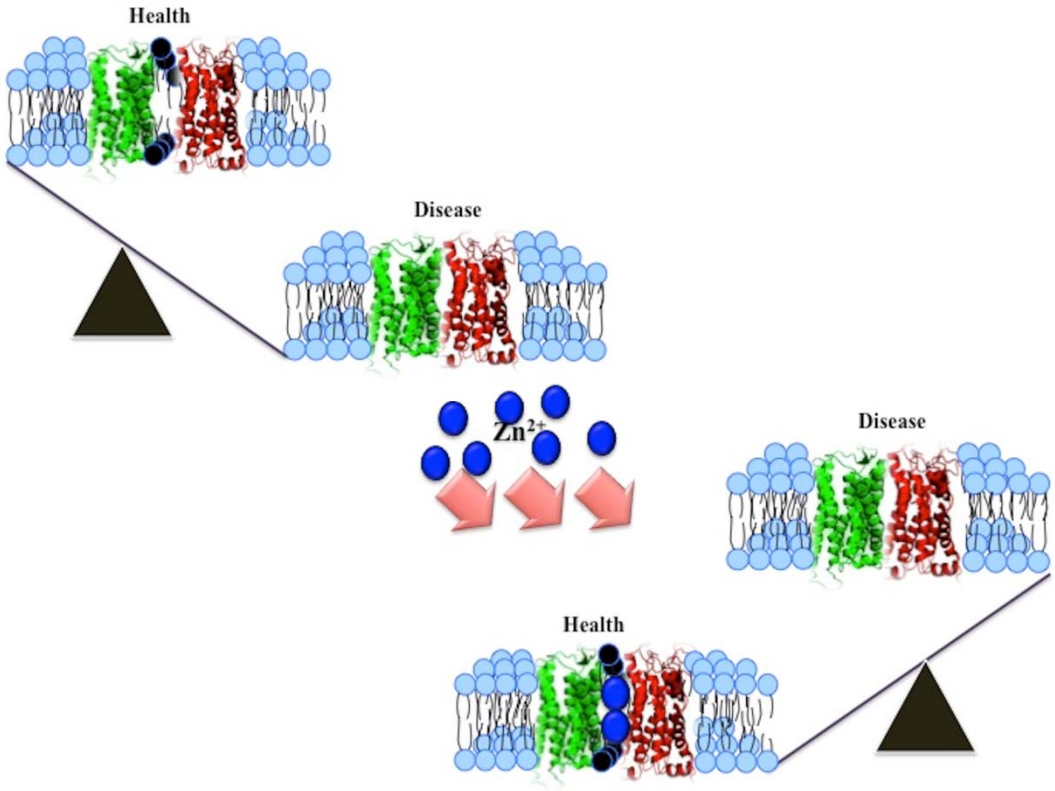

Figure 8